ACS OMEGA

http://pubs.acs.org/journal/acsodf

Open Access

This article is licensed under CC-BY 4.0

Article

A Switchable Deep Eutectic System Based on Diarylethene

Hugo Cruz,* Noémi Jordão, Sara Santiago, Silvia Mena, Andreia F. M. Santos, M. Teresa Viciosa, Karolina Zalewska, Luis C. Branco, Jordi Hernando,* and Gonzalo Guirado*

Cite This: *ACS Omega* 2025, 10, 50951−50961

Read Online

ACCESS | Metrics & More | Article Recommendations | Supporting Information

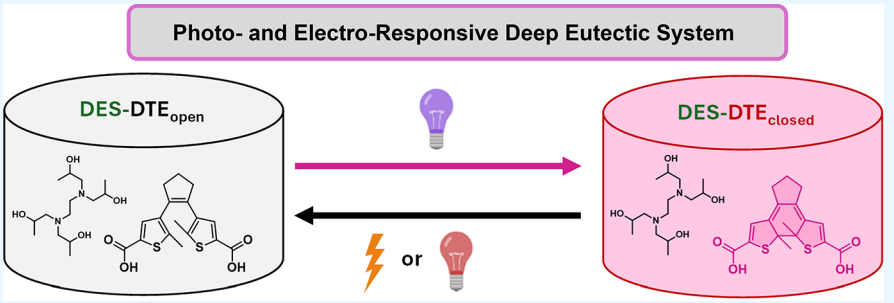

ABSTRACT: Deep eutectic solvents (DESs) have emerged as promising alternative solvents for a wide range of applications, such as extraction and separation processes. To broaden their functionality, the development of responsive DESs (RDESs) has attracted particular interest due to their ability to abruptly change their properties in response to external stimuli. Herein, we aim to prepare a new RDES comprising a photo- and electrochromic dicarboxylic diarylethene derivative (DTE) and quadrol (Q). The prepared system exhibits a color change from yellowish to pinkish-red under UV irradiation due to the photoisomerization of DTE, which can be reverted by visible light or oxidative electrolysis. Interestingly, this process also alters the strength of the hydrogen bonds between DTE and Q, leading to an externally controlled change in the thermal and electrical properties of the eutectic mixture. Therefore, these results demonstrate the capacity to photo- and electromodulate the behavior of DESs by incorporating stimuli-responsive units, thereby opening new perspectives toward the design of solvents with tunable properties for a variety of industrial and materials science applications.

Downloaded via 158.109.61.217 on December 10, 2025 at 18:16:05 (UTC).
See https://pubs.acs.org/sharingguidelines for options on how to legitimately share published articles.

INTRODUCTION

Currently, our society recognizes the need for more sustainable, eco-efficient, and eco-friendly chemical and engineering processes due to the intensive use of natural resources.[1] Considering that most chemical processes require the usage of conventional organic solvents, which can negatively impact pollution, energy consumption, air quality, and climate change, it is necessary to develop more sustainable solvents.[2] In this context, Pollet et al. proposed that "solvents must address simultaneously reaction efficiency, product separation and recyclability" to be considered competitive and environmentally conscious, contributing to the optimization of the overall process as well as its cost-effectiveness.[3,4]

In the past decades, different types of nonconventional solvents have been developed to meet these requirements. This is the case with switchable solvents (SSs), i.e., solvents that reversibly change their properties in response to an external stimulus (e.g., CO_2, pH, temperature), which have enabled improved reaction conditions as well as product separation for some selected processes.[3−5] For instance, one of the main applications of SSs is the development of CO_2-responsive systems, where CO_2 acts as a trigger to induce changes in the solvent properties, such as hydrophobicity and polarity, which can be exploited for a variety of applications.[6] More recently, another class of disruptive solvents has emerged that is composed of eutectic systems (ESs), as is the case for deep eutectic solvents (DESs). Usually, ESs are obtained by the complexation of a hydrogen-bond acceptor (HBA) and a hydrogen-bond donor (HBD), without additional purification steps.[7] These systems are an alternative to ionic liquids for the preparation of electrolytic media without the need for conventional organic solvents and supporting electrolytes, as they can combine rather high electrical conductivity with several additional advantages, such as easier preparation, eco-friendliness, and low-cost starting materials.[7,8−10] As a result, ESs and DESs are being explored in a wide range of applications, particularly in materials science, including electroplating and electrodeposition processes, electrocatalysis, supercapacitors and batteries, electrolytes for electrochromic

Received: May 8, 2025
Revised: September 26, 2025
Accepted: October 6, 2025
Published: October 21, 2025

© 2025 The Authors. Published by American Chemical Society

devices, photochromic nanocomposites, and bioinspired and responsive materials.[7,11−32]

To further expand the functionality of SSs and DESs, the development of new solvents that combine the best of both worlds has been proposed in recent years, giving rise to the so-called responsive DESs (RDESs), whose properties can be modulated with external stimuli.[33] This is the case for intrinsically electroresponsive DESs based on viologen derivatives, which behave as multifunctional materials that can act as both electrolytes and electrochromogens in electrochromic devices.[12]

Another very relevant stimulus for the preparation of responsive systems is light, which is used for manipulating the behavior of several photochromic materials currently exploited in ophthalmics (e.g., commercially available light-responsive lenses for sunglasses), photo-optical switching devices (e.g., optical memories, sensors, color switches, encryption/decryption devices, and actuators or molecular machines), light filters, as well as in textile, dyes, and cosmetic industries.[34,35] All these materials undergo a color change upon light excitation due to the reversible photoinduced transformation between two different states, which not only modifies their absorption spectra but also other physical and chemical properties.[36] Among the different light-responsive molecular systems designed to achieve this behavior, diarylethenes (DAEs) stand out, as they exhibit reversible photochemical reactivity, even in the solid state, with high efficiency, fatigue resistance, and low thermal reversibility, which can be tuned by modifying the functional groups introduced.[37,38] In particular, DAEs undergo a 6π-electron photocyclization reaction from their initial open isomer, generally colorless, to the colored closed state that is promoted by irradiation with UV light, i.e., ring-closure process. Then, back-photoisomerization takes place under visible light irradiation through a photocycloreversion reaction—i.e., ring-opening process.[38,39] Besides light, the cyclization and/or cycloreversion reactions of DAEs can also be promoted by electrochemical oxidation or reduction processes, a redox-switchable behavior that is highly dependent on the substituents present on the DAE moiety.[40−48]

Inspired by these attractive features of diarylethenes, in this work, we report their use for the preparation of a novel stimuli-responsive ES (ES-1), whose chemical, thermal, and electrical properties can be modulated with light and redox potentials. To achieve this goal, two different components were mixed in ES-1: *N*,*N*,*N*′,*N*′-tetrakis (2-hydroxypropyl)ethylenediamine, known as quadrol (Q), as a hydrogen bond acceptor; and a photoelectrochromic DAE-based dicarboxylic acid (DTE) as a hydrogen bond donor, which contains a switchable dithienylethene core (Figure 1). Interestingly, DTE is a Brønsted acid whose acidity/ability to form hydrogen bonds can be tuned with light and electrons due to the change in electronic communication that occurs between the two external carboxylic acid groups upon photoisomerization: they are insulated from each other in the open state and become selectively conjugated in the closed isomer, which has been reported to cause an increase in acidity after photocyclization.[49,50] As a result, switching between the open and closed isomers of DTE should reversibly modulate its hydrogen bonding interactions with Q, thus modifying the physicochemical properties of ES-1. It is worth mentioning that the ability of these responsive deep eutectic solvents (RDESs) to reversibly change color, polarity, and hydrogen bonding strength under photochemical or electrochemical stimuli makes them ideal candidates for the selective and tunable extraction of target compounds, for their use as active electrolytes in electrochromic devices, or for the on-demand modulation of catalytic activity and selectivity—paving the way for more efficient and controllable chemical processes.

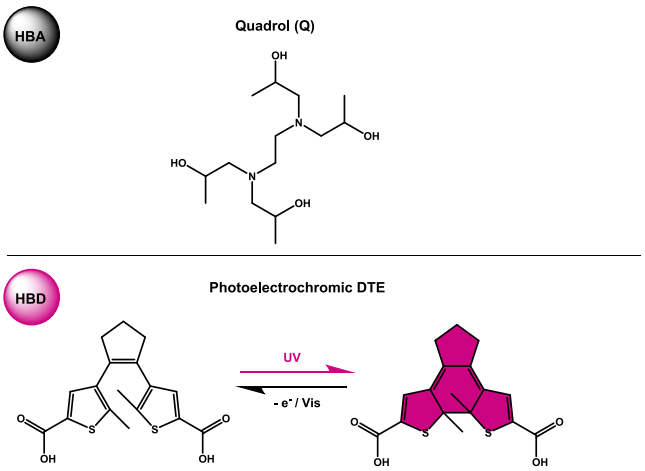

Figure 1. Chemical structures of HBA and HBD selected to form ES-1.

EXPERIMENTAL SECTION

Chemicals. *N*,*N*,*N*′,*N*′-Tetrakis (2-hydroxypropyl)-ethylenediamine (Q, > 98%), methanol (MeOH), and acetonitrile (ACN, puriss. electrochemical grade) were acquired from Sigma-Aldrich and used without further purification. Tetrabutylammonium hexafluorophosphate ([TBA]PF_6 puriss. electrochemical grade) was purchased from Fluka and dried overnight at 80 °C before use. The photoelectrochromic diacid 1,2-bis(5′-carboxy-2′-methylthien-3′-yl)-cyclopentene (DTE) was synthesized according to the procedures previously reported by us.[48,51]

Preparation of the Eutectic System, ES-1. To prepare ES-1, 1 equiv of DTE and 12 equiv of Q were stirred at 60 °C for 8 h until a yellowish viscous liquid was obtained. ^{1}H NMR (400.13 MHz, MeOD, 25 °C): δ = 7.38 (s, 2H) 3.37−3.33 (m, 48H), 3.00−2.29 (m, 144H), 1.82 (s, 6H), 1.14−1.11 (m, 144H) ppm.

Characterization of the Eutectic System, ES-1. *^{1}H Nuclear Magnetic Resonance (^{1}H NMR).* ^{1}H NMR spectra were recorded on a Bruker AMX400 spectrometer using MeOD as a deuterated solvent, and the chemical shifts were reported upfield in parts per million.

Differential Scanning Calorimetry (DSC). Thermal studies were carried out using a DSC Q2000 from TA Instruments Inc. (Tzero DSC technology) coupled to an RCS 90 cooling system and operating in the Heat Flow T4P option. Measurements were performed under anhydrous conditions, purged with 50 mL min^{-1} of high-purity nitrogen flow. DSC Tzero apparatus calibration was done in the temperature range between −90 and 200 °C. Enthalpy (cell constant) and temperature calibration were based on the melting peak of the indium standard (T_m = 156.60 °C) supplied by TA Instruments (lot number: E10W029). For each experiment, the samples were first dried under vacuum. Then, ∼4−7 mg were weighed and encapsulated in a hermetic Tzero aluminum pan and lid. All capsules were sealed before the analysis, and

https://doi.org/10.1021/acsomega.5c04216
ACS Omega 2025, 10, 50951−50961

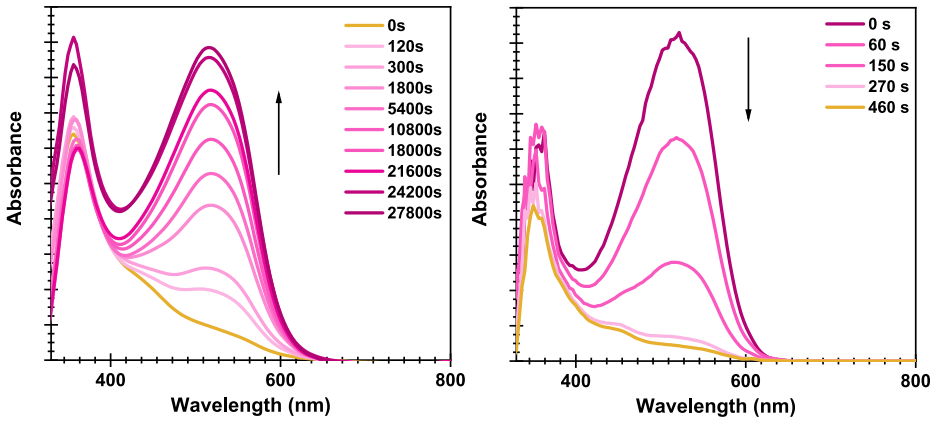

Figure 2. UV−vis absorption spectra of neat ES-1 until the PSS is reached after irradiation at: (left) 365 nm (27800 s) and (right) 532 nm (460 s). Measurements were conducted by depositing a thin layer of neat ES-1 (thickness ∼250 μm) on top of a transparent support.

the respective lids were perforated to prevent pressure build-up due to water evaporation. The experimental procedure consisted of first equilibrating all samples at 20 °C before subjecting them to several cooling and heating runs between −90 and 120 °C. Three scans at 10 °C min^{-1} were conducted to remove adsorbed water, record the phase transformations, and confirm the results obtained in the second run. Moreover, cooling/heating cycles at 5 °C min^{-1} and 20 °C min^{-1} were also performed. Data treatment was carried out through Universal Analysis 2000 software by TA Instruments Inc.

Dielectric Spectroscopy (DS). The electrical conductivity of Q and ES-$1_{open/closed}$ was studied by Dielectric Spectroscopy (DS). The samples were placed between two stainless steel electrodes (10 mm diameter) in a BDS 1200 parallel plate capacitor, with two 50 μm silica spacers used to maintain the sample thickness. The sample cell was mounted on a BDS 1100 cryostat. Temperature control was ensured by a Quatro Cryosystem controller and maintained to be within ±0.5 °C (all modules supplied by Novocontrol). Measurements were carried out using an Alpha-N analyzer from Novocontrol, covering a frequency range from 10^{-1} to 10^{6} Hz with an AC voltage of 1 [Vrms]. After a cooling ramp from 20 to −120 °C at 10 °C min^{-1}, a set of isothermal spectra was collected: from −120 to −50 °C, every 5 degrees; from −48 to 80 °C, every 2 degrees; and, finally, from 85 to 120 °C, every 5 degrees (exceptionally, for quadrol, spectra were also recorded every 5 degrees between 50 and 80 °C). This series corresponds to the "hydrated" state. Then, the samples were cooled again to −100 at 10 °C min^{-1}, and a second set of isothermal spectra was acquired in the same temperature steps. This second series corresponds to the "dried" state.

Photo- and Electrochemical Studies. Cyclic voltammetry (CV) measurements were carried out on a CH Instrument 660E potentiostat. All electrochemical studies in solution were performed using a platinum mesh and wire as the working and counter electrodes, respectively, and a saturated calomel electrode (SCE) as a reference electrode. The selected supporting electrolyte was a solution of acetonitrile (ACN) containing tetrabutylammonium hexafluorophosphate (0.1 M [TBA]PF_6). Additional CV measurements were conducted on screen-printed electrodes comprising ITO, carbon, and Ag as the working, counter, and pseudoreference electrodes, respectively. Optical parameters were determined by using spectroelectrochemical techniques. A VSP100 potentiostat was coupled to an L12090 Hamamatsu spectrophotometer; both instruments were controlled and synchronized using an EC-Lab V9.51 and Biokine 32 V. 4.46 software. The spectroelectrochemical experiments were performed using an electrochemical cell with 1 mm optical path length and applying controlled potential electrolysis; hence, a constant reduction potential was first applied, followed by a constant oxidation potential. The quantity of ES-1_{closed} photogenerated from ES-1_{open} was estimated by cyclic voltammetry performed in solution through the current intensity ratio between ES-1_{closed} and ES-1_{open}, which was normalized with the respective number of electrons involved in the corresponding electron transfer processes.

RESULTS AND DISCUSSION

Synthesis and Structural Analysis of the Eutectic System, ES-1. ES-1 was designed to be an intrinsically photo- and electrochromic material by selecting quadrol as HBA and the well-known photoelectrochromic diarylethene 1,2-bis(5′-carboxy-2′-methylthien-3′-yl)-cyclopentene as HBD. For ES-1 preparation, Q and DTE were mixed in a 12:1 molar ratio and stirred under heating (60 °C) for 8 h until a yellow viscous liquid was obtained. The initial feed ratio was preserved in the final material, as confirmed by ^{1}H NMR spectroscopy. It is important to note that no formation of a solid salt, resulting from acid−base reaction between the amino groups of Q and the carboxylic acid moieties of the open DTE unit, was observed. Instead, a pure liquid mixture was obtained. This suggests that the carboxylic acid groups may participate in hydrogen bonding interactions with Q, probably through both its hydroxyl and amino moieties.

Photo- and Electroinduced Responses of the Eutectic System, ES-1. To investigate whether the photoelectrochromic properties of DTE[49−51] were reproduced in ES-1, we conducted optical, electrochemical, and electro-optical studies in both solution (5:1 v/v ACN:MeOH, Figure S1) and neat (Figure 2) conditions. In its initial state, where DTE units remained in their open form (ES-1_{open}), ES-1 showed strong UV absorption and only a small absorption tail in the visible region, which provided a pale-yellow color to the neat system that was attenuated upon dilution. In contrast, irradiation with UV light (254 nm) induced a sudden coloration change to pink-red, characteristic of the closed DTE isomer, corresponding to the photocyclization of the DTE units of ES-1 (ES-1_{closed}). In particular, a new visible absorption band with maxima at 512 and 519 nm was recorded after UV irradiation

https://doi.org/10.1021/acsomega.5c04216
ACS Omega 2025, 10, 50951−50961

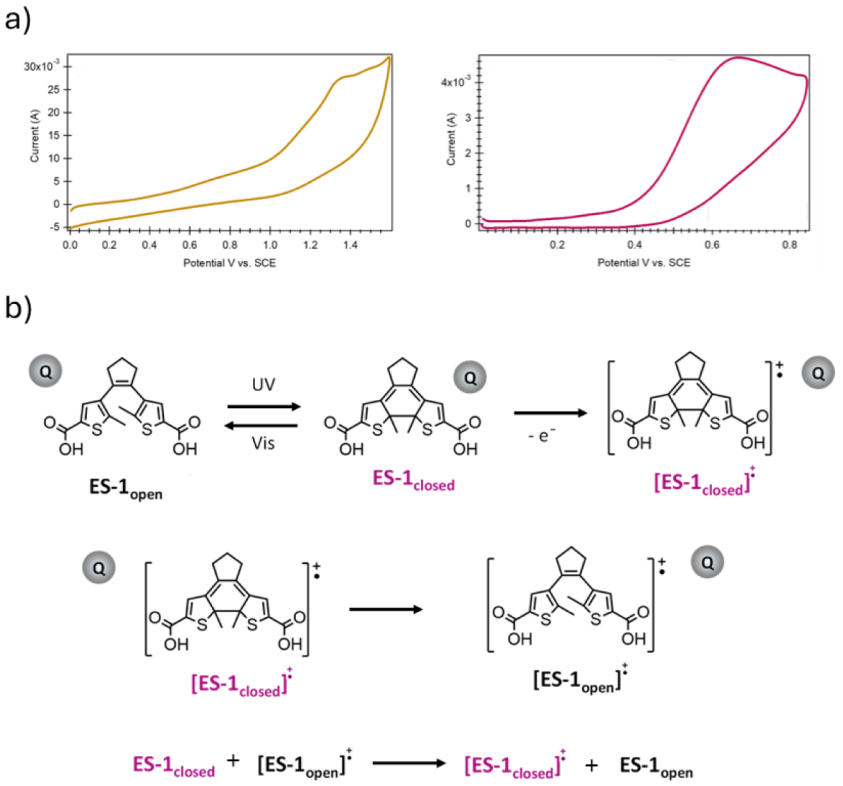

Figure 3. a) Cyclic voltammograms of a 3 mM solution of ES-1_{open} (left) and ES-1_{closed} (right) in ACN:MeOH (5:1 v/v) + 0.1 M [TBA]PF_6 at 0.2 $V{\cdot}s^{-1}$, comprising the 0/1.5/0 electrochemical window. The measurements were performed under N_2 atmosphere in a 3-electrode configuration device, where platinum wire, platinum grid, and saturated calomel electrode were used as working, counter, and reference electrodes, respectively. ES-1_{closed} was prepared by previous irradiation of ES-1_{open} at 254 nm, which produced a PSS with around 31% of closed DTE units, according to the intensity of their oxidation wave at E_{pa} = 0.66 V vs SCE. b) Scheme of the photo- and electrochemical isomerization process for the DTE unit of ES-1, where Q represents the quadrol moiety.

for the dissolved and neat ES-1, respectively (Figures 2 and S1), which resembles the behavior reported for pure DTE.[49−51] It should be highlighted that ES-1_{closed}, generated under these conditions, was not only composed of closed DTE units. Instead, a photostationary mixture was obtained, containing both open and closed DTE moieties, as also occurs for most diarylethenes.[52] The composition of such mixtures typically depends on the excitation wavelength and the solvent. However, other experimental conditions, including concentration, are also important in our case, as the high amount of DTE units in neat ES-1 limits UV light penetration and, therefore, photocyclization efficiency in the absence of stirring. Interestingly, the formation of ES-1_{closed} can be reverted upon further irradiation with visible light to photoexcite the closed DTE units of the system (532 nm), which undergo light-induced ring-opening to recover the initial ES-1 state (Figures 2 and S1).

According to the literature, DTE closed-to-open isomerization can also be triggered by electrochemical oxidation, which produces the corresponding radical cation of the closed isomer that spontaneously ring-opens to form the radical cation of the open state and eventually gets reduced to regenerate DTE_{open}.[49−51] These precedents prompted us to study the electrochromic behavior of ES-1 in solution and under neat conditions. To do so, the electrochemical properties of ES-1_{open} and ES-1_{closed} were investigated using cyclic voltammetry, enabling the determination of the potentials at which redox-induced ES-1_{closed} ring-opening should be conducted. Figure 3a shows the cyclic voltammogram of both states of ES-1, which were measured in solution with a supporting electrolyte (ACN/MeOH (5:1 v/v) + 0.1 M [TBA]PF_6). For ES-1_{open}, a chemical irreversible two-electron oxidation wave[48] was observed in the anodic region with a peak potential at E_{pa} = 1.33 V vs SCE. In agreement with the literature,[49,51] an irreversible one-electron oxidation wave was registered at much lower potentials for ES-1_{closed} (E_{pa} = 0.66 V vs SCE), which can promote the ring-opening process of its DTE units (Figure 3b).

In light of these results, we explored the electroisomerization of ES-1_{closed} under oxidation potentials, which were chosen to be higher than that of E_{pa} of ES-1_{closed} (to trigger radical ion formation of its DTE_{closed} moieties) and lower than that of E_{pa} of ES-1_{open} (to prevent DTE_{open} degradation by oxidation). To monitor the redox-induced transformation of ES-1_{closed}, spectroelectrochemical studies were performed, allowing the recording of the UV−vis absorption spectra during continuous oxidation. As shown in Figure 4, efficient color bleaching of ES-1_{closed} was observed upon oxidation in both solution ($E_{applied}$ = 1.0 V vs SCE) and neat conditions ($E_{applied}$ = 1.1 V vs SCE), a behavior that is consistent with redox-promoted ring opening of the closed DTE units in ES-1_{closed}. This conclusion was corroborated by subsequent irradiation with UV light, which resulted in recoloration of these samples due to photocyclization of the open DTE moieties regenerated upon oxidation. It must be noted that redox-induced ES-1_{closed} back-isomerization took much longer under neat conditions (2800 s) than in solution (65 s), as expected due to the higher concentration of DTE units. Despite this, full recovery of the

https://doi.org/10.1021/acsomega.5c04216
ACS Omega 2025, 10, 50951−50961

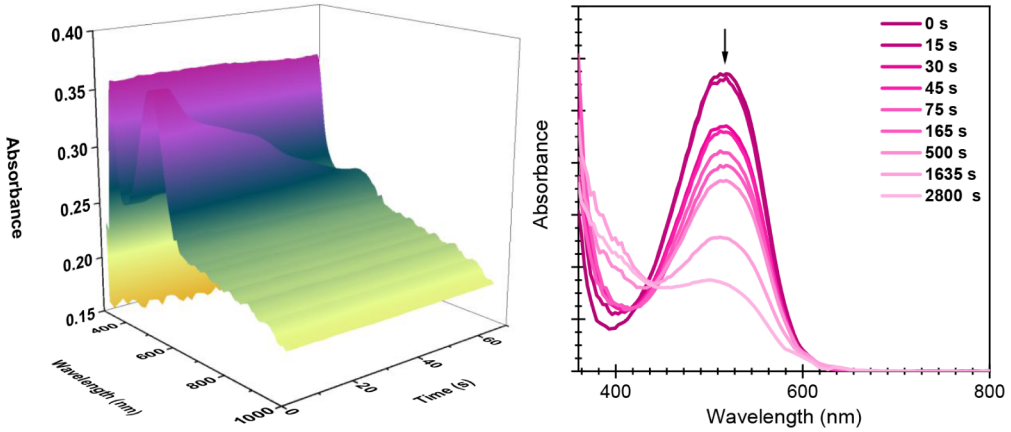

Figure 4. (Left) 3D graphical representation of the variation of the absorption spectrum of ES-1_{closed} (c = 3 mM) in ACN/MeOH (5:1 v/v) + 0.1 M [TBA]PF_6 solution when a constant potential of 1.0 V vs SCE was applied for 65 s. (Right) Variation of the UV−vis absorbance spectrum of neat ES-1_{closed} when a constant potential of 1.1 V vs SCE was applied for 2800 s.

Table 1. Photo- and Electrochemical Parameters for ES-1 and DTE[49,50] in ACN Solutions

	ES-1		DTE		
Isomer	E_{pa} (V) vs SCE		Protonation state	E_{pa} (V) vs SCE[51]	
Open	1.33		DTE	1.44	
			DTE-COO^-	1.12	
			DTE-$2COO^-$	0.87	
	E_{pa} (V) vs SCE	$\lambda_{abs,max}$ (nm)		E_{pa} (V) vs SCE[49]	$\lambda_{abs,max}$ (nm)[50]
Closed	0.66	512	DTE	0.85	536
			DTE-COO^-	0.57	533
			DTE-$2COO^-$	0.33	498

initial ES-1_{open} absorbance was not observed, even after such a long electrolytic time, suggesting that the rate of the redox-induced ring-opening process is significantly slow. Regarding the long-term reversibility of this ES in response to light or redox stimuli, no significant degradation of the sample was detected after several cycles of stimulation. The robustness of this photoelectrochromic diarylethene system can be attributed to the fully reversible and self-regenerating nature of its photochemical and electrochemical processes. Upon UV irradiation, the molecule switches from a colorless open form to a colored closed form, which reverts under visible light without structural degradation. The closed form can also be electrochemically oxidized to a radical cation, reopening spontaneously. Then, this open-ring radical cation can be reduced back to the neutral open form via an intermolecular electron transfer reaction with closed isomer molecules (Figure 3b). This redox cycle prevents the accumulation of degradation products and ensures that reactive intermediates are short-lived, resulting in a self-regenerating system suitable for long-term applications.

Although the photo- and electrochromic behavior observed for ES-1 was similar to that previously described for DTE,[49,50] some significant differences were identified in terms of absorbance (closed-state $\lambda_{abs,max}$ in the visible region) and electrochemical parameters (E_{pa}), as summarized in Table 1. This table also includes the $\lambda_{abs,max}$ and E_{pa} values previously reported for the three protonation states of pure DTE, namely, its diacid (DTE), monocarboxylate (DTE-COO^-) and dicarboxylate (DTE-$2COO^-$) forms, which slightly vary with the deprotonation degree of DTE.[49,50]

The analysis of the E_{pa} values revealed a reduction in the peak oxidation potential of DTE in ES-1 relative to the pure diacid DTE, with a decrease of 8% for DTE_{open} and 22% for DTE_{closed}. These findings indicate that the carboxylic groups of DTE interact significantly with the complementary moieties of Q in the closed state of ES-1, a behavior that is in agreement with the light-induced modulation of acidity previously reported for DTE.[50] In particular, the acidity of pure DTE_{closed} was reported to be higher than that of DTE_{open}, with 25- and 10-fold increments in the K_a acidity constant of their first and second ionization processes. Consequently, the hydrogen-bond donor capacity of the carboxylic acid groups of DTE should also increase upon photocyclization, thus accounting for the stronger interaction of DTE_{closed} with Q in ES-1. In other words, the introduction of the photoelectrochromic DTE unit into ES-1 allows modulation of the supramolecular interactions within the eutectic mixture, which might influence the thermal and electrical properties of the system.

Thermal Analysis by Differential Scanning Calorimetry of the Eutectic System, ES-1. To investigate the effect of DTE isomerization on the thermal behavior of ES-1, DSC measurements were performed for neat Q, ES-1_{open} and ES-1_{closed}. The latter was obtained through a previous photocyclization reaction of ES-1_{open}, which leads to an equilibrium photostationary state (PSS) where both DTE_{open} and DTE_{closed} isomers coexist, as mentioned earlier. As a result, the differences that could be observed in the thermal properties of ES-1_{open} and ES-1_{closed} must be taken as a lower limit of the actual modulation amplitude between the fully open and closed forms of ES-1.

https://doi.org/10.1021/acsomega.5c04216
ACS Omega 2025, 10, 50951−50961

Figure 5 illustrates the thermograms obtained for ES-1_{open} and ES-1_{closed} in the second heating run after water removal, as

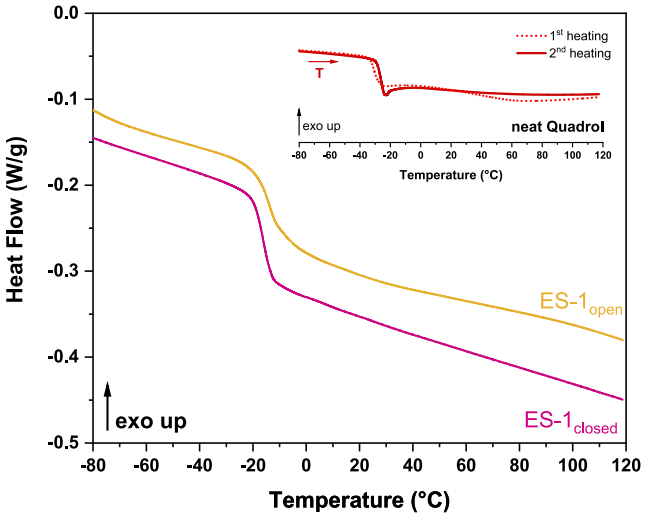

Figure 5. DSC curves obtained at 10 °C min^{-1} for dried ES-1_{open} and ES-1_{closed} (2nd heating run). Inset: thermograms of neat Q (1st and 2nd heating runs).

well as for neat Q (first and second heating runs), which is the major component of the eutectic mixture. For the first heating cycle of neat Q (see inset of Figure 5), a glass transition process was observed at $T_{g\text{-onset}}$ = −33.4 °C, followed by an endothermal event associated with water evaporation (T = 20−120 °C). Removal of water caused the glass transition of Q to shift to higher temperatures ($T_{g\text{-onset}}$ = −28.8 °C) in the subsequent cooling and heating runs, which demonstrates the glass-forming ability of this compound and indicates that water acts as a plasticizer when it is hydrated. A similar thermal behavior was observed for the two states of ES-1: the addition of DTE to Q did not result in the appearance of other thermal events in the eutectic mixture, apart from a single glass transition process. Therefore, this suggests that both ES-1_{open} and ES-1_{closed} correspond to homogeneous mixtures of Q and DTE that also produce vitreous states upon cooling—a thermal response that was found to be independent of the heating and cooling rates tested (5, 10, and 20 °C min^{-1}), with no visible degradation of the mixture up to 120 °C.

However, some significant differences can be detected between the DSC thermograms of Q and the two forms of ES-1, which are also illustrated by the thermal parameters given in Table 2: $T_{g\text{-onset}}$ values and the heat capacity change (ΔC_p) measured for the first (hydrated samples) and second heating (dried samples) cycles of neat Q, ES-1_{open}, and ES-1_{closed}. On the one hand, we observed that the glass transition registered for dried Q presents an accentuated relaxation enthalpy, which is typically associated with the release of degrees of freedom upon heating that normally occurs after the sample has been in a nonequilibrium state below its glass transition temperature.[53] In contrast, neither dried ES-1_{open} nor dried ES-1_{closed} exhibited such a relaxation enthalpy when T_g is exceeded under the same experimental conditions. This result suggests that the eutectic mixtures have a higher resistance to physical aging in their glassy state, which could originate from a more compact—i.e., less free volume—or rigid structure, probably due to Q−DTE interactions. The latter could also explain the differences measured for $T_{g\text{-onset}}$ between Q and the two isomers of ES-1. In particular, an increment of about 10 °C was registered for dried ES-1_{open} and ES-1_{closed} relative to neat Q, which may indicate that the additional hydrogen bonds between Q and DTE in these mixtures stabilize their glassy phase. As a result, more thermal energy would be required to activate their molecular motion through glass transition.

Regarding the comparison between ES-1_{open} and ES-1_{closed}, much smaller differences in $T_{g\text{-onset}}$ were determined (∼1 °C), which are within the error margin of our measurements. More significant differences were observed for the ΔC_p value associated with the glass transition of ES-1_{open} and ES-1_{closed}: 0.51 J (g °C)$^{-1}$ vs 0.73 J (g °C)$^{-1}$, respectively. Such a variation suggests that ES-1_{closed} presents a more ordered glassy state as it gains more degrees of freedom with the glass transition. This observation could be correlated with two main factors: (i) the stronger hydrogen bonds expected between DTE_{closed} and Q according to the electro-optical measurements discussed above, and (ii) the structural changes associated with the isomerization of DTE, as DTE_{closed} exhibits a rigid conjugated planar structure that should enable additional $\pi-\pi$ stacking interactions[54] to take place in the glassy state of ES-1_{closed}. In light of this, an even more compact and ordered molecular arrangement should be expected for ES-1_{closed} relative to ES-1_{open}, which leads to a measurable variation in the thermal properties upon reversible photoisomerization between these two states.

Electrical Properties by Dielectric Spectroscopy (DS) of the Eutectic System, ES-1. *Electrical Conductivity.* Similar to the thermal behavior, the effect of DTE isomerization on the conductivity profiles was also investigated through Dielectric Spectroscopy (DS) experiments for neat Q, ES-1_{open}, and ES-1_{closed}, assessing the frequency and temperature dependence of complex electrical conductivity $\sigma^*(\omega,T)$ and impedance $Z^*(\omega,T)$, in which both properties comprise a real and an imaginary component.[55,56]

In particular, the real part of complex electrical conductivity is related to charge migration, while the imaginary part corresponds to charge storage.[57,58] In general, semiconducting disordered materials, such as DESs, exhibit a common profile

Table 2. Temperatures ($T_{g\text{-onset}}$) and Heat Capacity Variations (ΔC_p) for the Glass Transition Detected on the First (Hydrated Samples) and Second Heating (Dried Samples) Runs of Neat Q, ES-1_{open}, and ES-1_{closed}[a]

Compound	Hydrated (1st heating run)		Dried (2nd heating run)		Water content (%)[b]
	$T_{g\text{-onset}}$ (°C)	ΔC_p (J (g·°C)$^{-1}$)	$T_{g\text{-onset}}$ (°C)	ΔC_p (J (g°C)$^{-1}$)	
Q	−33.4	0.73	−28.8	0.75	0.10
ES-1_{open}	−30.4	0.66	−18.7	0.51	6.24
ES-1_{closed}	−28.1	0.71	−19.6	0.73	2.51

[a] $T_{g\text{-onset}}$ was defined as the onset of heat flow change. [b] The water content was estimated from the percentage of weight lost during the first calorimetric run.

https://doi.org/10.1021/acsomega.5c04216
ACS Omega 2025, 10, 50951−50961

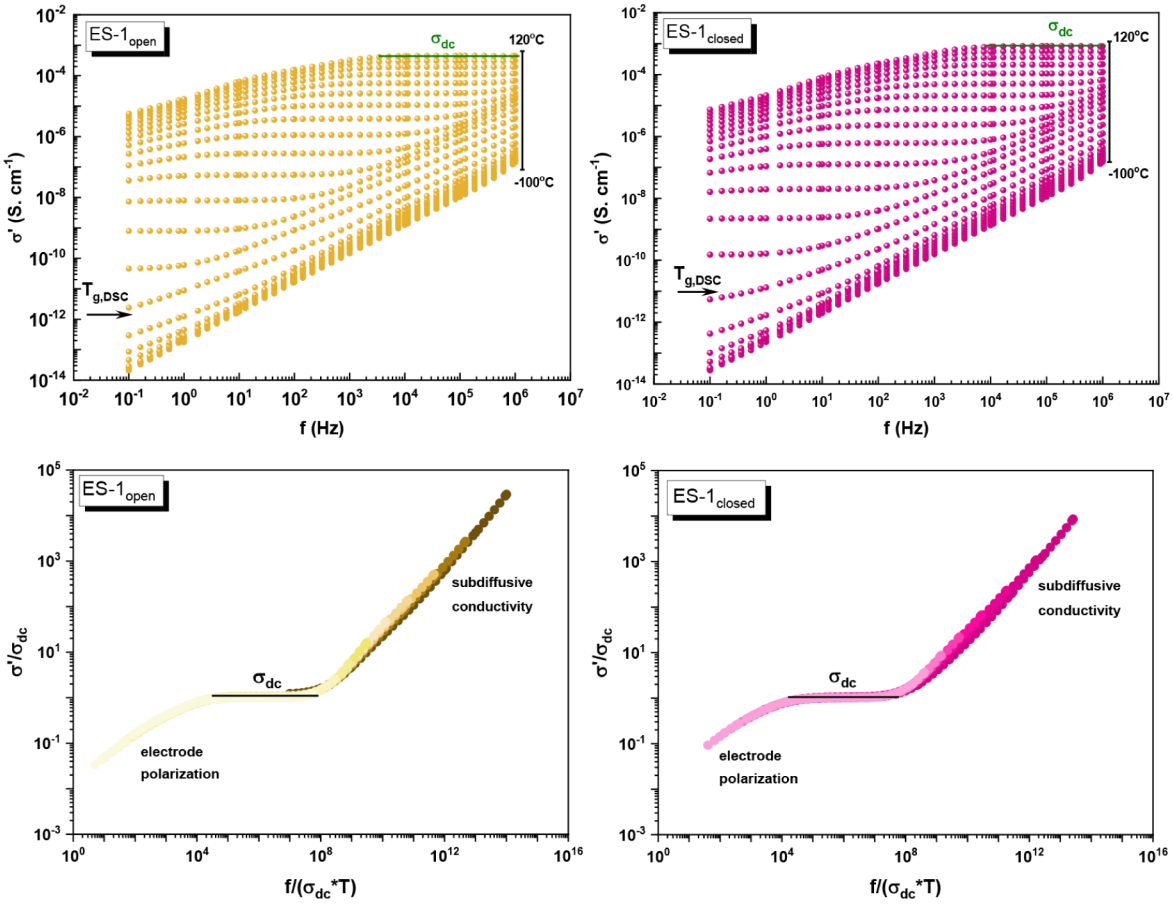

Figure 6. Real part of the complex conductivity (σ') spectra and the master curves scaled, according to Summerfield equation, for dried ES-1_{open} and ES-1_{closed}.

Table 3. σ_{dc} at T_g, DSC and 25 °C, Applicable Temperature Range for Jonscher's Equation, VFTH Fit Parameters, and Fragility Index

		Jonscher's data			VFTH fit parameters			
	Compound	σ_{dc} ($T_{g,DSC}$) [S cm^{-1}]	σ_{dc} (25 °C) [S cm^{-1}]	[T_i;T_e][a] [°C]	σ_∞[S cm^{-1}]	B [K]	T_0 [K]	m[b]
Hydrated	Q	2.0×10^{-14}	2.3×10^{-8}	[−22; 100]	0.4	2163.1	169.3	38
	ES-1_{open}	2.8×10^{-12}	9.1×10^{-6}	[−32; 38]	70.8	2070.5	168.2	51
	ES-1_{closed}	3.9×10^{-7}	3.3×10^{-4}	[−60; 10]	37.2	1732.1	149.9	52
Dried	Q	1.0×10^{-14}	2.2×10^{-8}	[−16; 100]	0.5	2003.3	179.5	41
	ES-1_{open}	6.0×10^{-13}	1.4×10^{-7}	[−14; 80]	55.0	2440.6	175.7	47
	ES-1_{closed}	1.0×10^{-11}	3.2×10^{-7}	[−16; 52]	28.8	2176.5	179.8	49

[a] T_i—Initial temperature and T_e—end temperature represent the selected temperature range to carry out the experiment. [b] Fragility index estimated at $\sigma(1/T) = 5 \times 10^{-13}$ S cm^{-1}.

for the real conductivity (σ') plots, presenting different regimes that may or may not be frequency dependent.[55] At lower temperatures and higher frequencies, σ' depends on frequency, corresponding to a short-distance subdiffusive charge transport mechanism (alternating current conductivity) through back-and-forth motion over limited ranges.[26,59−61] As temperature increases, a frequency-independent regime emerges as a plateau (direct current conductivity (σ_{dc}) value), indicating the transition to a diffusive regime due to long-distance charge migration.[26,59−61]

For all of the samples, DS measurements were performed in both hydrated and dried states, the latter being obtained after a thermal treatment at 120 °C for 1 h. Figure 6 displays the conductivity spectra, collected from −100 to 120 °C, for dried ES-1_{open} and ES-1_{closed}, while the data for their hydrated states and neat Q are plotted in Figures S2−S4.

Similar to our previous works with DESs,[14,26] the plateau in the σ' plot of hydrated and dried ES-1_{open} as well as dried ES-1_{closed} was only observed at temperatures above the calorimetric glass transition ($T_{g,DSC}$) (see arrow in Figure 6), indicating a relationship between the cooperative motions of the dynamical glass transition and the transport mechanism that governs the diffusive regime (σ_{dc}).[59,62] However, this behavior was not observed for hydrated ES-1_{closed}. At higher temperatures and lower frequencies, for both samples in hydrated and dried states, a reduction of σ' value is detected with the decrease in frequency, as charge carriers accumulate at the electrodes' surface without discharging.[56,60] This phenom-

https://doi.org/10.1021/acsomega.5c04216
ACS Omega 2025, 10, 50951−50961

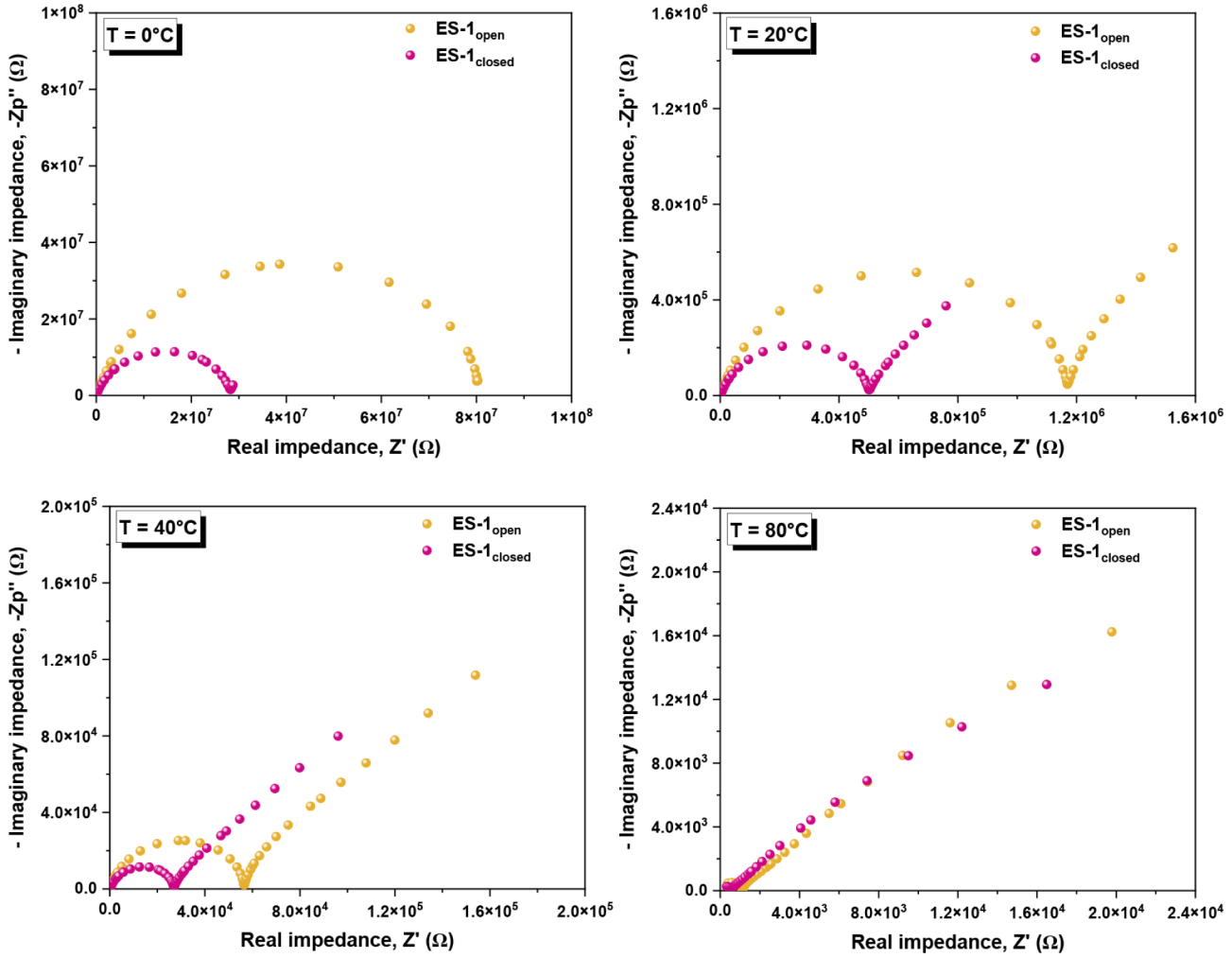

Figure 7. Nyquist plots for dried ES-1_{open} and ES-1_{closed} at different temperatures: 0 °C, 20 °C, 40 °C, and 80 °C.

enon is called electrode polarization. Furthermore, the obtained σ' spectra for each material, acquired at different temperatures, can be superimposed according to the Summerfield master plot. This allows for better distinction between each above-mentioned regime in the respective conductivity profile (see Figure 6, bottom plots).[63]

Another relevant parameter to be considered in such materials is the fragility index (m), which describes the degree of curvature based on the steepness of the temperature dependence at T_g (Equation S3). For this parameter, higher m values indicate a greater variation in viscosity and conductivity with temperature at T_g. Materials can be classified as strong ($m \sim 16$) or fragile ($m \geq \sim 200$), depending on whether their transport properties resist more or less against temperature changes, respectively.[64]

Table 3 summarizes the σ_{dc} at T_g and at 25 °C, as well as the temperature range for which it was possible to use Jonscher's equation, VFTH fit parameters, and the fragility index (m).

Foreseeing future applications at room temperature, it can be useful to compare the results at T = 25 °C. In this context, higher conductivity values were observed for both hydrated and dried ES-$1_{open/closed}$ when compared to neat Q. In the hydrated state, ES-1_{closed} exhibits higher conductivity than ES-1_{open}, a difference that becomes more pronounced at T_g. At this temperature, the σ_{dc} of ES-1_{closed} is 5 orders of magnitude higher when compared with the open-ring isomer, despite both isomers having comparable estimated water contents. Thus, water plays an important role, not so much associated with its content but with how the charge transport is assured. It is important to note that well below T_g, when ES-1_{closed} is in the glassy state, long-distance charge migration still occurs, pointing to a water-assisted charge transport mechanism. In the case of the dried isomers, the σ_{dc} value of ES-1_{closed} (3.2×10^{-7} S cm^{-1}) is two times higher than ES-1_{open} (1.4×10^{-7} S cm^{-1}).

Considering that hydrated ES-1_{closed} exhibited anomalous conductivity behavior with respect to the location of its glass transition temperature, the fragility index (m, Equation S3) was instead determined from the steepness of $\sigma(1/T)$, at a fixed conductivity value of 5×10^{-13} S cm^{-1}, to standardize the estimation criterion. This value represents the average conductivity measured at T_g for the other compounds, closely aligning with the *ad hoc* value identified by Leys et al. for a series of methylimidazolium ionic liquids.[65] Furthermore, the m values obtained for both hydrated and dried samples allow us to classify these systems as strong glass formers.

Nyquist Plots. To gain a better understanding of the impact of DTE isomerization on relevant electrical properties for the development of electronic devices, additional studies were conducted by using impedance data obtained from dielectric measurements. Indeed, the frequency and temperature dependence of the complex electrical impedance ($Z^*(\omega,T)$)

https://doi.org/10.1021/acsomega.5c04216
ACS Omega 2025, 10, 50951−50961

provide information related to the electrical properties of the material and electrolyte/electrode interface.[66] The so-called Nyquist plot, in which the symmetric of the imaginary part is plotted as a function of the real one, can exhibit two distinct regions: (i) at high frequencies, a semicircle, related to bulk ionic conduction, emerges, and (ii) at low frequencies, a tail is detected due to the electrode polarization effect.[67,68]

The Nyquist plots measured for dried ES-1_{open} and ES-1_{closed} at different temperatures are presented in Figure 7, while the data for neat Q are given in Figures S7 and S8. For temperatures above the glass transition, it is possible to observe a semicircle, whose diameter decreases with increasing temperature, indicating that the resistance to charge migration is reduced. With the increase in temperature, a tail associated with electrode polarization starts to emerge, which is more evident in this type of plot compared to isothermal spectra. More importantly, at the same temperature, dried ES-1_{closed} showed a lower semicircle diameter—i.e., lower resistance—than ES-1_{open}, allowing better charge transport across the bulk electrolyte. Therefore, this result corroborates the conclusion that the electrical conductivity of ES-1 can be photo- and electromodulated upon DTE isomerization, thereby illustrating the ability to tune the properties of deep eutectic solvents through the application of external stimuli.

CONCLUSIONS

Smart responsive systems are attracting special interest due to their capacity to abruptly change their properties in response to external stimuli, such as light and electrical currents. Herein, we aim to prepare a new responsive system based on deep eutectic solvents, comprising a photo- and electrochromic dicarboxylic diarylethene derivative and quadrol. The prepared system reveals a variation in coloration from yellowish to pink-red under UV irradiation due to the photoisomerization of DTE, which can be reverted with visible light or oxidative electrolysis. Interestingly, this process also alters the strength of the hydrogen bond between DTE and Q, resulting in an externally controlled change in the thermal and electrical properties of the eutectic mixture. Indeed, calorimetric analyses showed that ES-1_{open} and ES-1_{closed} are good glass formers, suggesting that the hydrogen bonds between Q and DTE in these mixtures stabilize their glassy phase, vitrifying at higher temperatures compared to neat Q. Notably, a significant difference in heat capacity was observed between the two isomers of ES-1, indicating that ES-1_{closed} exhibits a more ordered glassy state, as it gains more degrees of freedom with the transition from the glassy to the supercooled liquid phase. Moreover, according to dielectric data, ES-1_{closed} also showed higher electrical conductivities than ES-1_{open}, both at cryogenic temperatures slightly above the glass transition and at room temperature. These results were corroborated by Nyquist plots, where ES-1_{closed} presented a lower resistance, suggesting that it allows better charge transport across the bulk electrolyte than ES-1_{open}. Overall, this work demonstrates the potential of developing stimuli-responsive eutectic mixtures, as the external control of their physicochemical properties—e.g., color, conductivity—can find applications in a wide range of fields, such as smart solvent systems for extraction and separation and switchable catalysis. In this sense, the ability of these responsive deep eutectic solvents (RDESs) to reversibly alter color, polarity, and hydrogen bonding strength under photochemical or electrochemical stimuli could be used not only for the selective and tunable extraction of target compounds but also to modulate catalytic activity or selectivity on demand, paving the way for more efficient and controllable chemical processes.

ASSOCIATED CONTENT

Supporting Information

The Supporting Information is available free of charge at https://pubs.acs.org/doi/10.1021/acsomega.5c04216.

Experimental techniques used to characterize the eutectic system. These comprise photo- and electro-induced response measurements, electrical properties by dielectric spectroscopy, and impedance characterization through Nyquist plots (PDF)

AUTHOR INFORMATION

Corresponding Authors

Hugo Cruz − *LAQV-REQUIMTE, Department of Chemistry, NOVA School of Science and Technology, NOVA University of Lisbon, Caparica 2829-516, Portugal; INL − International Iberian Nanotechnology Laboratory, Braga 4715-330, Portugal;* orcid.org/0000-0002-1047-7342; Email: hugogdsc@gmail.com

Jordi Hernando − *Departament de Química, Universitat Autònoma de Barcelona, Cerdanyola Del Vallès, Barcelona 08193, Spain;* orcid.org/0000-0002-1126-4138; Email: jordi.hernando@uab.cat

Gonzalo Guirado − *Departament de Química, Universitat Autònoma de Barcelona, Cerdanyola Del Vallès, Barcelona 08193, Spain;* orcid.org/0000-0003-2128-7007; Email: gonzalo.guirado@uab.cat

Authors

Noémi Jordão − *Departament de Química, Universitat Autònoma de Barcelona, Cerdanyola Del Vallès, Barcelona 08193, Spain*

Sara Santiago − *Departament de Química, Universitat Autònoma de Barcelona, Cerdanyola Del Vallès, Barcelona 08193, Spain*

Silvia Mena − *Departament de Química, Universitat Autònoma de Barcelona, Cerdanyola Del Vallès, Barcelona 08193, Spain*

Andreia F. M. Santos − *LAQV-REQUIMTE, Department of Chemistry, NOVA School of Science and Technology, NOVA University of Lisbon, Caparica 2829-516, Portugal;* orcid.org/0000-0002-9395-3112

M. Teresa Viciosa − *Centro de Química Estrutural, Institute of Molecular Sciences, Instituto Superior Técnico, University of Lisbon, Lisbon 1049-001, Portugal;* orcid.org/0000-0002-8574-7351

Karolina Zalewska − *LAQV-REQUIMTE, Department of Chemistry, NOVA School of Science and Technology, NOVA University of Lisbon, Caparica 2829-516, Portugal*

Luis C. Branco − *LAQV-REQUIMTE, Department of Chemistry, NOVA School of Science and Technology, NOVA University of Lisbon, Caparica 2829-516, Portugal;* orcid.org/0000-0003-2520-1151

Complete contact information is available at: https://pubs.acs.org/10.1021/acsomega.5c04216

Notes

The authors declare no competing financial interest.

■ ACKNOWLEDGMENTS

The authors are grateful for financial support from the Ministerio de Ciencia, Innovación y Universidades of Spain MICIU/AEI/10.13039/501100011033 and the ERDF—"A way of making Europe" through projects PID2022-141293OB-I00 and TED2021-130797B-I00. AGAUR/Generalitat de Catalunya through projects 2021 SGR 00052 and 2021 SGR 00064. This work was also supported by the Associate Laboratory for Green Chemistry LAQV-REQUIMTE (UID/50006/2023) and CQE (UIDB/00100/2020, UIDP/00100/2020, LA/P/0056/2020UIDB/00100/2020), as well as the projects PTDC/QUI-QOR/7450/2020—"Organic Redox Mediators for Energy Conversion" and MIT-EXPL/CS/0055/2021 funded by the Portuguese Foundation for Science and Technology (MCTES). A.F.M.S. acknowledges FCT-MCTES for the PhD Grant (SFRH/BD/132551/2017). S.M. and S.S. acknowledge support from the postdoctoral grant Juan de la Cierva funding and the European Union "NextGenerationEU"/PRTR. Finally, H.C. and M.T.V. thank financial support within the scope of the framework contract foreseen in numbers 4, 5, and 6 of article 23 of the Decree-Law 57/2016 of 29 August, as amended by Law 57/2017 of 19 July. J.H. is a Serra Húnter Professor.

■ REFERENCES

(1) Lozano, F. J.; Lozano, R.; Freire, P.; Jiménez-Gonzalez, C.; Sakao, T.; Ortiz, M. G.; Trianni, A.; Carpenter, A.; Viveros, T. New Perspectives for Green and Sustainable Chemistry and Engineering: Approaches from Sustainable Resource and Energy Use, Management, and Transformation. *J. Cleaner Prod.* **2018**, *172*, 227−232.

(2) Clarke, C. J.; Tu, W.-C.; Levers, O.; Bröhl, A.; Hallett, J. P. Green and Sustainable Solvents in Chemical Processes. *Chem. Rev.* **2018**, *118* (2), 747−800.

(3) Pollet, P.; Eckertabc, C. A.; Liotta, C. L. Switchable Solvents. *Chem. Sci.* **2011**, *2* (4), 609−614.

(4) Pollet, P.; Davey, E. A.; Ureña-Benavides, E. E.; Eckert, C. A.; Liotta, C. L. Solvents for Sustainable Chemical Processes. *Green Chem.* **2014**, *16* (3), 1034−1055.

(5) Jessop, P. G.; Heldebrant, D. J.; Li, X.; Eckert, C. A.; Liotta, C. L. Reversible Nonpolar-to-Polar Solvent. *Nature* **2005**, *436* (7054), 1102−1102.

(6) Jessop, P. G.; Mercer, S. M.; Heldebrant, D. J. CO2-Triggered Switchable Solvents, Surfactants, and Other Materials. *Energy Environ. Sci.* **2012**, *5* (6), 7240−7253.

(7) Smith, E. L.; Abbott, A. P.; Ryder, K. S. Deep Eutectic Solvents (DESs) and Their Applications. *Chem. Rev.* **2014**, *114* (21), 11060−11082.

(8) Abbott, A. P.; Boothby, D.; Capper, G.; Davies, D. L.; Rasheed, R. K. Deep Eutectic Solvents Formed between Choline Chloride and Carboxylic Acids: Versatile Alternatives to Ionic Liquids. *J. Am. Chem. Soc.* **2004**, *126* (29), 9142−9147.

(9) Abbott, A. P.; Capper, G.; Davies, D. L.; Rasheed, R. K.; Tambyrajah, V. Novel Solvent Properties of Choline Chloride/Urea Mixtures. *Chem. Commun.* **2003**, *1*, 70−71.

(10) Florindo, C.; Oliveira, F. S.; Rebelo, L. P. N.; Fernandes, A. M.; Marrucho, I. M. Insights into the Synthesis and Properties of Deep Eutectic Solvents Based on Cholinium Chloride and Carboxylic Acids. *ACS Sustainable Chem. Eng.* **2014**, *2* (10), 2416−2425.

(11) Zhang, C.; Ding, Y.; Zhang, L.; Wang, X.; Zhao, Y.; Zhang, X.; Yu, G. A Sustainable Redox-Flow Battery with an Aluminum-Based, Deep-Eutectic-Solvent Anolyte. *Angew. Chem., Int. Ed.* **2017**, *56* (26), 7454−7459.

(12) Cruz, H.; Jordão, N.; Dionísio, M.; Pina, F.; Branco, L. C. Intrinsically Electrochromic Deep Eutectic Solvents. *ChemistrySelect* **2019**, *4* (4), 1530−1534.

(13) Goeltz, J. C.; Matsushima, L. N. Metal-Free Redox Active Deep Eutectic Solvents. *Chem. Commun.* **2017**, *53* (72), 9983−9985.

(14) Cruz, H.; Jordão, N.; Amorim, P.; Dionísio, M.; Branco, L. C. Deep Eutectic Solvents as Suitable Electrolytes for Electrochromic Devices. *ACS Sustainable Chem. Eng.* **2018**, *6* (2), 2240−2249.

(15) Miller, M. A.; Wainright, J. S.; Savinell, R. F. Iron Electrodeposition in a Deep Eutectic Solvent for Flow Batteries. *J. Electrochem. Soc.* **2017**, *164* (4), A796−A803.

(16) Gurkan, B.; Squire, H.; Pentzer, E. Metal-Free Deep Eutectic Solvents: Preparation, Physical Properties, and Significance. *J. Phys. Chem. Lett.* **2019**, *10* (24), 7956−7964.

(17) Sakita, A. M. P.; Della Noce, R.; Fugivara, C. S.; Benedetti, A. V. On the Cobalt and Cobalt Oxide Electrodeposition from a Glyceline Deep Eutectic Solvent. *Phys. Chem. Chem. Phys.* **2016**, *18* (36), 25048−25057.

(18) Jordão, N.; Cruz, H.; Pina, F.; Branco, L. C. Studies of Bipyridinium Ionic Liquids and Deep Eutectic Solvents as Electrolytes for Electrochromic Devices. *Electrochim. Acta* **2018**, *283*, 718−726.

(19) Cruz, H.; Jordão, N.; Branco, L. C. Deep Eutectic Solvents (DESs) as Low-Cost and Green Electrolytes for Electrochromic Devices. *Green Chem.* **2017**, *19* (7), 1653−1658.

(20) Mukesh, C.; Gupta, R.; Srivastava, D. N.; Nataraj, S. K.; Prasad, K. Preparation of a Natural Deep Eutectic Solvent Mediated Self Polymerized Highly Flexible Transparent Gel Having Super Capacitive Behaviour. *RSC Adv.* **2016**, *6* (34), 28586−28592.

(21) Mondal, D.; Sharma, M.; Wang, C.-H.; Lin, Y.-C.; Huang, H.-C.; Saha, A.; Nataraj, S. K.; Prasad, K. Deep Eutectic Solvent Promoted One Step Sustainable Conversion of Fresh Seaweed Biomass to Functionalized Graphene as a Potential Electrocatalyst. *Green Chem.* **2016**, *18* (9), 2819−2826.

(22) Chakrabarti, M. H.; Mjalli, F. S.; AlNashef, I. M.; Hashim, M. A.; Hussain, M. A.; Bahadori, L.; Low, C. T. J. Prospects of Applying Ionic Liquids and Deep Eutectic Solvents for Renewable Energy Storage by Means of Redox Flow Batteries. *Renewable Sustainable Energy Rev.* **2014**, *30*, 254−270.

(23) Bhatt, J.; Mondal, D.; Bhojani, G.; Chatterjee, S.; Prasad, K. Preparation of Bio-Deep Eutectic Solvent Triggered Cephalopod Shaped Silver Chloride-DNA Hybrid Material Having Antibacterial and Bactericidal Activity. *Mater. Sci. Eng.* **2015**, *56*, 125−131.

(24) Ejeromedoghene, O.; Zuo, X.; Oderinde, O.; Yao, F.; Adewuyi, S.; Fu, G. Photochromic Behavior of Inorganic Superporous Hydrogels Fabricated from Different Reacting Systems of Polymeric Deep Eutectic Solvents. *J. Mol. Struct.* **2023**, *1271*, 134101.

(25) Ejeromedoghene, O.; Ma, X.; Oderinde, O.; Yao, F.; Adewuyi, S.; Fu, G. Quaternary Type IV Deep Eutectic Solvent-Based Tungsten Oxide/Niobium Oxide Photochromic and Reverse Fading Composite Complex. *New J. Chem.* **2021**, *45* (38), 18008−18018.

(26) Cruz, H.; Jordao, N.; Pinto, A. L.; Dionisio, M.; Neves, L. A.; Branco, L. C. Alkaline Iodide-Based Deep Eutectic Solvents for Electrochemical Applications. *ACS Sustainable Chem. Eng.* **2020**, *8* (29), 10653−10663.

(27) Nahar, Y.; Horne, J.; Truong, V.; Bissember, A. C.; Thickett, S. C. Preparation of Thermoresponsive Hydrogels via Polymerizable Deep Eutectic Monomer Solvents. *Polym. Chem.* **2021**, *12* (2), 254−264.

(28) Florindo, C.; Celia-Silva, L. G.; Martins, L. F. G.; Branco, L. C.; Marrucho, I. M. Supramolecular Hydrogel Based on a Sodium Deep Eutectic Solvent. *Chem. Commun.* **2018**, *54* (54), 7527−7530.

(29) Zhang, H.; Gao, T.; Zhang, S.; Zhang, P.; Li, R.; Ma, N.; Wei, H.; Zhang, X. Conductive and Tough Smart Poly(N-Isopropylacrylamide) Hydrogels Hybridized by Green Deep Eutectic Solvent. *Macromol. Chem. Phys.* **2021**, *222* (1), 2000301.

(30) Wu, R.; Liu, K.; Ren, J.; Yu, Z.; Zhang, Y.; Bai, L.; Wang, W.; Chen, H.; Yang, H. Cellulose Nanocrystals Extracted from Grape Pomace with Deep Eutectic Solvents and Application for Self-Healing Nanocomposite Hydrogels. *Macromol. Mater. Eng.* **2020**, *305* (3), 1900673.

(31) Oderinde, O.; Ejeromedoghene, O.; Fu, G. Synthesis and Properties of Low-Cost, Photochromic Transparent Hydrogel Based

https://doi.org/10.1021/acsomega.5c04216
ACS Omega 2025, 10, 50951−50961

on Ethaline-Assisted Binary Tungsten Oxide-Molybdenum Oxide Nanocomposite for Optical Memory Applications. *Polym. Adv. Technol.* **2022**, *33* (3), 687−699.
(32) Tomé, L. C.; Mecerreyes, D. Emerging Ionic Soft Materials Based on Deep Eutectic Solvents. *J. Phys. Chem. B* **2020**, *124* (39), 8465−8478.
(33) Zhang, M.; Zhang, Z.; Gul, Z.; Tian, M.; Wang, J.; Zheng, K.; Zhao, C.; Li, C. Advances of Responsive Deep Eutectic Solvents and Application in Extraction and Separation of Bioactive Compounds. *J. Sep. Sci.* **2023**, *46* (15), 2300098.
(34) Moretti, C.; Tao, X.; Koehl, L.; Koncar, V.Electrochromic Textile Displays for Personal Communication. In *Smart Textiles And Their Applications*; Woodhead Publishing, 2016, pp. 539−568.
(35) Nunes, D.; Pimentel, A.; Santos, L.; Barquinha, P.; Pereira, L.; Fortunato, E.; Martins, R. Chromogenic Applications. In *Metal Oxide Nanostructures*; Elsevier, 2019, pp. 103−147.
(36) Bamfield, P.; Hutchings, M. *Chromic Phenomena: Technological Applications of Colour Chemistry*, Bamfield, P.; Hutchings, M., Eds.; The Royal Society of Chemistry, 2018, DOI: 10.1039/9781788012843.
(37) Irie, M. Diarylethenes for Memories and Switches. *Chem. Rev.* **2000**, *100* (5), 1685−1716.
(38) Irie, M.; Fukaminato, T.; Matsuda, K.; Kobatake, S. Photochromism of Diarylethene Molecules and Crystals: Memories, Switches, and Actuators. *Chem. Rev.* **2014**, *114* (24), 12174−12277.
(39) Matsuda, K.; Irie, M. Diarylethene as a Photoswitching Unit. *J. Photochem. Photobiol., C* **2004**, *5* (2), 169−182.
(40) Gorodetsky, B.; Branda, N. R. Bidirectional Ring-Opening and Ring-Closing of Cationic 1,2-Dithienylcyclopentene Molecular Switches Triggered with Light or Electricity. *Adv. Funct. Mater.* **2007**, *17* (5), 786−796.
(41) Gorodetsky, B.; Samachetty, H. D.; Donkers, R. L.; Workentin, M. S.; Branda, N. R. Reductive Electrochemical Cyclization of a Photochromic 1,2-Dithienylcyclopentene Dication. *Angew. Chem., Int. Ed.* **2004**, *43* (21), 2812−2815.
(42) Baron, R.; Onopriyenko, A.; Katz, E.; Lioubashevski, O.; Willner, I.; Wang, S.; Tian, H. An Electrochemical/Photochemical Information Processing System Using a Monolayer-Functionalized Electrode. *Chem. Commun.* **2006**, *20*, 2147−2149.
(43) Browne, W. R.; de Jong, J. J. D.; Kudernac, T.; Walko, M.; Lucas, L. N.; Uchida, K.; van Esch, J. H.; Feringa, B. L. Oxidative Electrochemical Switching in Dithienylcyclopentenes, Part 2: Effect of Substitution and Asymmetry on the Efficiency and Direction of Molecular Switching and Redox Stability. *Chem. Eur. J.* **2005**, *11* (21), 6430−6441.
(44) Moriyama, Y.; Matsuda, K.; Tanifuji, N.; Irie, S.; Irie, M. Electrochemical Cyclization/Cycloreversion Reactions of Diarylethenes. *Org. Lett.* **2005**, *7* (15), 3315−3318.
(45) Peters, A.; Branda, N. R. Electrochemically Induced Ring-Closing of Photochromic 1,2-Dithienylcyclopentenes. *Chem. Commun.* **2003**, *8*, 954−955.
(46) Guirado, G.; Coudret, C.; Launay, J.-P. Electrochemical Remote Control for Dithienylethene-Ferrocene Switches. *J. Phys. Chem. C* **2007**, *111* (6), 2770−2776.
(47) Zhou, X.-H.; Zhang, F.-S.; Yuan, P.; Sun, F.; Pu, S.-Z.; Zhao, F.-Q.; Tung, C.-H. Photoelectrochromic Dithienylperfluorocyclopentene Derivatives. *Chem. Lett.* **2004**, *33* (8), 1006−1007.
(48) Guirado, G.; Coudret, C.; Hliwa, M.; Launay, J.-P. Understanding Electrochromic Processes Initiated by Dithienylcyclopentene Cation-Radicals. *J. Phys. Chem. B* **2005**, *109* (37), 17445−17459.
(49) Massaad, J.; Micheau, J.-C.; Coudret, C.; Serpentini, C. L.; Guirado, G. Proton Catalysis in the Redox Responsivity of a Mini-Sized Photochromic Diarylethene. *Chem. Eur. J.* **2013**, *19* (37), 12435−12445.
(50) Massaad, J.; Micheau, J.-C.; Coudret, C.; Sanchez, R.; Guirado, G.; Delbaere, S. Gated Photochromism and Acidity Photomodulation of a Diacid Dithienylethene Dye. *Chem. Eur. J.* **2012**, *18* (21), 6568−6575.
(51) Jordão, N.; Ferreira, P.; Cruz, H.; Parola, A. J.; Branco, L. C. Photochromic Room Temperature Ionic Liquids Based on Anionic Diarylethene Derivatives. *ChemPhotochem* **2019**, *3* (7), 525−528.
(52) Herder, M.; Schmidt, B. M.; Grubert, L.; Pätzel, M.; Schwarz, J.; Hecht, S. Improving the Fatigue Resistance of Diarylethene Switches. *J. Am. Chem. Soc.* **2015**, *137* (7), 2738−2747.
(53) Vyazovkin, S.; Koga, N.; Schick, C. *Handbook of Thermal Analysis and Calorimetry: Recent Advances, Techniques And Applications*; Elsevier, 2018; Vol: 6, 1-842.
(54) Higashiguchi, K.; Taira, G.; Kitai, J. I.; Hirose, T.; Matsuda, K. Photoinduced Macroscopic Morphological Transformation of an Amphiphilic Diarylethene Assembly: Reversible Dynamic Motion. *J. Am. Chem. Soc.* **2015**, *137* (7), 2722−2729.
(55) Kremer, F.; Różański, S. A. The Dielectric Properties of Semiconducting Disordered Materials. In *Broadband Dielectric Spectroscopy*; Springer: Berlin, Heidelberg, 2003, pp. 475−494.
(56) Iacob, C.; Sangoro, J. R.; Serghei, A.; Naumov, S.; Korth, Y.; Kärger, J.; Friedrich, C.; Kremer, F. Charge Transport and Glassy Dynamics in Imidazole-Based Liquids. *J. Chem. Phys.* **2008**, *129* (23), 234511.
(57) Abdul Halim, S. I.; Chan, C. H.; Apotheker, J. Basics of Teaching Electrochemical Impedance Spectroscopy of Electrolytes for Ion-Rechargeable Batteries - Part 2: Dielectric Response of (Non-) Polymer Electrolytes. *Chem. Teach. Int.* **2021**, *3* (2), 117−129.
(58) Chan, C. H.; Kammer, H.-W. Characterization of Polymer Electrolytes by Dielectric Response Using Electrochemical Impedance Spectroscopy. *Pure Appl. Chem.* **2018**, *90* (6), 939−953.
(59) Carvalho, T.; Augusto, V.; Brás, A. R.; Lourenço, N. M. T.; Afonso, C. A. M.; Barreiros, S.; Correia, N. T.; Vidinha, P.; Cabrita, E. J.; Dias, C. J.; Dionísio, M.; Roling, B. Understanding the Ion Jelly Conductivity Mechanism. *J. Phys. Chem. B* **2012**, *116* (9), 2664−2676.
(60) Dyre, J. C.; Maass, P.; Roling, B.; Sidebottom, D. L. Fundamental Questions Relating to Ion Conduction in Disordered Solids. *Rep. Prog. Phys.* **2009**, *72* (4), 046501.
(61) Santos, A. F. M.; Figueirinhas, J. L.; Dias, C. J.; Godinho, M. H.; Branco, L. C.; Dionísio, M. Study of the Mesomorphic Properties and Conductivity of *N*-Alkyl-2-Picolinium Ionic Liquid Crystals. *J. Mol. Liq.* **2023**, *377*, 121456.
(62) Carvalho, T.; Augusto, V.; Rocha, Â.; Lourenço, N. M. T.; Correia, N. T.; Barreiros, S.; Vidinha, P.; Cabrita, E. J.; Dionísio, M. Ion Jelly Conductive Properties Using Dicyanamide-Based Ionic Liquids. *J. Phys. Chem. B* **2014**, *118* (31), 9445−9459.
(63) Summerfield, S. Universal Low-Frequency Behaviour in the a.c. Hopping Conductivity of Disordered Systems. *Philos. Mag. B* **1985**, *52* (1), 9−22.
(64) Böhmer, R.; Ngai, K. L.; Angell, C. A.; Plazek, D. J. Nonexponential Relaxations in Strong and Fragile Glass Formers. *J. Chem. Phys.* **1993**, *99* (5), 4201−4209.
(65) Leys, J.; Wübbenhorst, M.; Preethy Menon, C.; Rajesh, R.; Thoen, J.; Glorieux, C.; Nockemann, P.; Thijs, B.; Binnemans, K.; Longuemart, S. Temperature Dependence of the Electrical Conductivity of Imidazolium Ionic Liquids. *J. Chem. Phys.* **2008**, *128* (6), 064509.
(66) Aziz, S. B. Occurrence of Electrical Percolation Threshold and Observation of Phase Transition in Chitosan (1−x): AgI x ($0.05 \leq x \leq 0.2$)-Based Ion-Conducting Solid Polymer Composites. *Appl. Phys. A: Mater. Sci. Process* **2016**, *122* (7), 706.
(67) Aziz, S. B.; Faraj, M. G.; Abdullah, O. G. Impedance Spectroscopy as a Novel Approach to Probe the Phase Transition and Microstructures Existing in CS: PEO Based Blend Electrolytes. *Sci. Rep.* **2018**, *8* (1), 1−14308.
(68) Frömling, T.; Kunze, M.; Schönhoff, M.; Sundermeyer, J.; Roling, B. Enhanced Lithium Transference Numbers in Ionic Liquid Electrolytes. *J. Phys. Chem. B* **2008**, *112* (41), 12985−12990.

https://doi.org/10.1021/acsomega.5c04216
ACS Omega 2025, 10, 50951−50961